

Fuel Properties and Combustion Kinetics of Hydrochar Prepared by Hydrothermal Carbonization of Corn Straw

Xianjun Xing,^{a,b,*,#} Fangyu Fan,^{a,c,d,#} Suwei Shi,^a Yongqiang Xing,^a Yongling Li,^a Xuefei Zhang,^a and Jing Yang^a

The potential of using hydrothermal carbonization (HTC) on corn straw (CS) was studied for the production of solid fuel. The effects of hydrothermal conditioning on the mass yield, energy yield, higher heating value (HHV), H/C and O/C atomic ratios, the morphology, and equilibrium moisture content (EMC) of hydrochars were examined by varying the reaction temperature (170 °C, 200 °C, 230 °C, and 260 °C) and the residence time (15 min and 30 min). The results demonstrated that the solid fuel properties of hydrochar produced at 230 °C for 30 min had an appropriate HHV of 20.51 MJ/kg, a mass yield of 64.80%, and an energy yield of 77.41%. The physical structure changed because of hydrothermal carbonization and the hydrophobicity of hydrochar increased in comparison to raw corn straw after hydrothermal carbonization. The combustion characteristics and kinetic parameters of raw corn straw and hydrochar were calculated based on the thermogravimetric curves according to Arrhenius equation. The activation energies of hydrochars were larger than that of raw corn straw. The comprehensive combustibility index (S) of raw corn straw was greater than that of hydrochar when the reaction temperature and residence time were 230 °C and 30 min, respectively.

Keywords: Corn straw; Hydrothermal carbonization; Hydrochar; Fuel properties; Combustion characteristics; Kinetic parameters

Contact information: a: Advanced Energy Technology and Equipment Research Institute, Hefei University of Technology, Hefei, Anhui 230009, PR China; b: National City Energy Measurement center (Anhui), Hefei, Anhui 230009, PR China; c: The College of Forestry, Southwest Forestry University, Kunming, Yunnan 650224, PR China; d: School of Chemistry and Chemical Engineering, Hefei University of Technology, Hefei, Anhui 230009, PR China;

*Corresponding author: xxianjun@hfut.edu.cn, #: these authors contributed equally to this study.

INTRODUCTION

With the increasing demand for fossil fuel and the growing environmental pollution caused by CO₂, NO_x, and SO₂ emissions from burning fossil fuel, sustainable energy sources are attracting attention worldwide, specifically biomass conversion (Lou *et al.* 2014; Valverde *et al.* 2016). Biomass is a type of abundant renewable energy that is low in sulfur and NO_x emissions during combustion. However, the utilization of biomass is limited because of the natural drawbacks, such as high moisture content, hygroscopic nature, and low energy density. Presently, various techniques (*i.e.*, carbonization, gasification, and liquefaction) have been successfully applied to generate denser and more transportable energy products from different forms of biomass, reducing the dependence on fossil energy (Ma *et al.* 2012; Abnisa *et al.* 2014; Thangalazhy-Gopakumar *et al.* 2015).

Hydrothermal carbonization is currently one of the most interesting processes for biomass thermo-chemical conversion. The raw materials are surrounded by water and kept in a liquid state by allowing the pressure to rise with steam pressure. With increasing process temperatures and corresponding pressure up to a certain degree, most biomass still remains, with very little gas and liquid generated (Libra *et al.* 2011). Compared with other techniques, hydrothermal carbonization has some remarkable benefits, such as simplicity, relatively mild reaction conditions, wide availability of raw materials, and less greenhouse gas emissions (Guo *et al.* 2015; Nizamuddin *et al.* 2015).

Up until now, research has investigated the hydrothermal carbonization of biomass. Gao *et al.* (2016) investigated the effects of biomass type and temperature with longer residence times, including the evaluation of physicochemical, pyrolytic, and combustion characteristics. Smith and Ross (2016) produced bio-coal, bio-methane, and fertilizer from seaweed via hydrothermal carbonization. Basso *et al.* (2016) pre-treated grape marc *via* the hydrothermal carbonization process to improve fuel properties, and the results showed that the hydrochar exhibited interesting higher heating value (HHV) and physical-chemical characteristics, which made hydrochar exploitable as a solid fuel. Jatzwauck and Schumpe (2015) analyzed hydrothermal carbonization of soft rush in the temperature range of 453 K to 513 K, using a kinetic model. Álvarez-Murillo *et al.* (2015) prepared hydrochar through hydrothermal carbonization using olive stone with the processing conditions of 1.1 to 12.3% biomass/water ratio, 150 to 250 °C, and a 3.2 h to 36.8 h residence time. The solid yield ranged from 30.95% to 55.75%, and the HHV ranged from 22.2 MJ/kg to 29.59 MJ/kg.

Corn straw is a type of the agriculture waste, totaling 250 million tons annually in China (Chen *et al.* 2008). Currently, corn straw is primarily disposed of by means of burning, which results in considerable environmental pollution. Compared with traditional means, biochars of corn straw, produced by thermo-chemical means, are promising because of their high content of lignocelluloses (Jin *et al.* 2014). There have been some reports about the pyrolysis mechanism and utilization of biochar of corn straw in soil amelioration (Zhao *et al.* 2014; Lu *et al.* 2015; Wang *et al.* 2015). However, literature on hydrochar produced from corn straw as solid fuel is limited. Fuertes *et al.* (2010) investigated the physical and chemical properties of hydrochar and biochar from corn stover through hydrothermal carbonization and pyrolysis, and analyzed differences in the char's properties. Xiao *et al.* (2012) addressed the physical and chemical properties of hydrochar from corn straw at the reaction temperature of 250 °C and a reaction time of 4 h. The treatment produced an increase in HHV of 29.2 MJ/kg, which was greater than 66.8% of the raw material. Guo *et al.* (2015) discussed the characteristic evolution of hydrochar from hydrothermal carbonization of corn straw. The literature revealed that the characteristics of hydrochar approached those of low grade coal (Fuertes *et al.* 2010; Xiao *et al.* 2012; Guo *et al.* 2015). Above all, the production ratios of hydrochar were lower when the reaction time greater than 3 h. Thus, higher production ratios requiring a shorter reaction time is proposed in this paper.

In addition, researchers (Wang *et al.* 2012; Fang *et al.* 2013) have investigated the combustion kinetic parameters of corn straw by thermogravimetric analysis (TGA). However, raw corn straw has natural drawbacks, such as high volatile material content and low energy density. In an attempt to overcome this drawback, corn straw was converted to hydrochar to improve the combustion behavior. Thus, research of the combustion kinetics of hydrochar is important. Meanwhile, TGA is a common method to evaluate the combustion behavior and kinetics of solid samples (Islam *et al.* 2016; Yang

et al. 2016). To the best of our knowledge, there have been no reports dealing with the combustion behavior and kinetics of hydrochar produced by the hydrothermal carbonization of corn straw.

The objectives of this experiment are as follows: (1) understand the fuel properties after hydrothermal carbonization over the temperature ranges of 170 °C to 260 °C and residence times of 15 min and 30 min; (2) explore the combustion behaviors and kinetics parameters of hydrochar from corn straw.

EXPERIMENTAL

Materials

The biomass used in this study was corn straw, obtained from Anhui province, China. The corn straw was shredded to shorter than 0.6 mm fractions and then dried at 105 °C for 24 h, followed by hydrothermal carbonization. The proximate and ultimate analyses are shown in Table 1.

Table 1. The Proximate and Ultimate Analyses of Corn Straw

Material	Proximate analysis					Ultimate analysis				
	Moisture (%)	Volatile (%)	Fixed carbon (%)	Ash (%)	HHV (MJ·kg ⁻¹)	C (%)	H (%)	O (%)	N (%)	S (%)
CS	4.90	72.15	17.07	5.88	17.17	43.30	5.95	49.42	1.21	0.12

Hydrochar Preparation

The hydrochar was prepared in a laboratory scale Hastelloy alloy batch reactor (Anhui Kemi Machinery Technology Co., Ltd., China), with a working volume of 50 mL, a maximum operating temperature of 370 °C, and a pressure of 22 MPa. Initially, approximately 5.0 g of corn straw powder was combined with 40 mL deionized water in a batch reactor. The reactor was flooded with nitrogen under high pressure to discharge oxygen from the reactor. This process was repeated 5 times. Next, the reactor was placed into a ceramic furnace with a digital temperature controller (Anhui Kemi Machinery Technology Co., Ltd., China). The reactor was maintained at the desired temperature, ranging from 170 °C to 260 °C for 15 min or 30 min. After the specified reaction time, the reactor was immediately immersed into water to cool down and stop the reaction. Finally, the mixture inside the reactor was filtered through a G-4 glass filter to obtain the solid product (hydrochar). The hydrochar was dried at 105 °C for 24 h and preserved hermetically. The hydrochar samples were designated as “CSXXX-YYY”, where CS referred to corn straw and “XXX” and “YYY” represented the temperature and the residence time, respectively.

Characteristics of Corn Straw and Hydrochar

Elemental contents (C, H, N, and S) of the corn straw and hydrochar were determined using a Vario Micro Cube elemental analyzer (Elementar, Germany). The higher heating values of the samples were measured according to the EN 14918 (Miranda *et al.* 2009) testing standard (combustion under pure oxygen atmosphere at 25 °C using an oxygen bomb calorimeter; Huadian Analysis Instrument Co., Ltd, China), calibrated

with benzoic acid. The mass and energy yields were calculated by Eq. (1) and Eq. (2) as follows:

$$\text{Mass yield (\%)} = (m_{\text{hydrochar}}/m_{\text{cs}}) \times 100 \quad (1)$$

$$\text{Energy yield (\%)} = (\text{HHV}_{\text{hydrochar}}/\text{HHV}_{\text{cs}}) \times \text{mass yield} \quad (2)$$

The samples were sputter-coated with Pt (Platinum, the aim is to increase the conductivity) for analysis by scanning electron microscopy (SEM), using a JSM-6490LV scanning electron microscope (JEOL, Japan).

The equilibrium moisture content (EMC) was determined by placing 20.0 g of each sample in two separate large bottles containing saturated sodium chloride and potassium carbonate, at the experimental temperature of 30 °C for 48 h. The relative humidity (RH) was approximately 75% and 42% in the two bottles, respectively. The EMC of the samples was calculated as the weight difference before and after treatment.

The combustion behavior of hydrochar was evaluated by thermogravimetric analysis (TGA) (Setaram, France) within a temperature range of ambient temperature to 900 °C, with different heating rates of 10 °C/min, 20 °C/min, and 40°C/min. The total gas flow rate was maintained at 60 mL/min (N₂: O₂ = 4:1). The sample was sieved, and particles, less than 0.075 μm in size, were tested. Approximately 10 ± 0.1 mg of each sample was used for the test.

Determination of the Kinetic Parameters of Corn Straw and Hydrochar during Combustion

Thermogravimetric analysis was used to analyze the combustion characteristics of corn straw and hydrochar. The kinetic parameters of combustion provide useful information for the design and optimization of thermo-chemical systems. Currently, there are many methods for calculating kinetic parameters (Sait *et al.* 2012; Yang *et al.* 2016). The reaction rate of the samples obeyed the fundamental Arrhenius equation (Eq. 3),

$$\frac{d\alpha}{dT} = \frac{A}{\beta} \exp\left(-\frac{E}{RT}\right)(1-\alpha)^n \quad (3)$$

where, A is the frequency or pre-exponential factor, E is the activation energy of the reaction, R is the universal gas constant, T is the absolute temperature, β is the heating rate, α is the thermal conversion fraction of the samples at time t , and n is the order of the reaction.

The degree of conversion, α , was defined by Eq. 4,

$$\alpha = \frac{m_0 - m_T}{m_0 - m_\infty} \quad (4)$$

where m_0 , m_T , and m_∞ , are the initial, actual, and final weights of the sample, respectively.

According to the Coats-Redfern method (Garcia *et al.* 2015), kinetic parameters are calculated according to the logarithmic expressions of Eq. 5 and Eq. 6.

$$\ln\left[\frac{1-(1-\alpha)^{1-n}}{T^2(1-n)}\right] = \ln\left[\frac{AR}{\beta E}\left(1-\frac{2RT}{E}\right)\right] - \frac{E}{RT} \quad (n \neq 1) \quad (5)$$

$$\ln\left[-\ln\left(\frac{1-\alpha}{T^2}\right)\right] = \ln\left[\frac{AR}{\beta E}\left(1-\frac{2RT}{E}\right)\right] - \frac{E}{RT} \quad (n = 1) \quad (6)$$

Given the temperature range and activation energies in this study, $RT/E < 1$ and $(1-2RT/E) \approx 1$, Eq. 5 and Eq. 6 were transformed as follows:

$$\ln\left[\frac{1-(1-\alpha)^{1-n}}{T^2(1-n)}\right] = \ln\frac{AR}{\beta E} - \frac{E}{RT} \quad (n \neq 1) \quad (7)$$

$$\ln\left[-\ln\frac{(1-\alpha)}{T^2}\right] = \ln\frac{AR}{\beta E} - \frac{E}{RT} \quad (n = 1) \quad (8)$$

The values of α and T were used to calculate the TGA. The plot of, $\ln\left[\frac{1-(1-\alpha)^{1-n}}{T^2(1-n)}\right]$ vs. $1/T$ ($n \neq 1$) or $\ln\left[-\ln\frac{(1-\alpha)}{T^2}\right]$ vs. $1/T$ ($n = 1$), represented a correlative straight line when the reaction order was selected appropriately. The activation energy was derived from the slope, and the pre-exponential factor A was calculated as the intercept of the straight line.

Calculation of the Comprehensive Combustibility Index

The comprehensive combustibility index determined the combustion reactivity of the samples (Wang *et al.* 2015), and was calculated according to Eq. 9,

$$S = \frac{(dw/dt)_{\max}(dw/dt)_{\text{mean}}}{T_i^2 T_h} \quad (9)$$

where $(dw/dt)_{\max}$ and $(dw/dt)_{\text{mean}}$ represent the maximum and mean rates of weight loss (wt./min), respectively, and T_i and T_h are the ignition and burnout temperatures.

RESULTS AND DISCUSSION

Effect of Hydrothermal Carbonization Temperature and Time on the Mass and Energy Yields of Hydrochar

The hydrothermal carbonization temperature and the residence time were the most important factors that affected the thermal stability of the samples. Table 2 shows the mass and energy yields of hydrochar, the elemental composition (C, H, O, N, and S) of the samples, and the HHV of hydrochars produced under various conditions.

The mass and energy yields of hydrochars followed a decreasing trend with increasing temperature, as shown in Table 2. The mass energy and energy yields ranged from 50.49% to 92.51% and 69.51% to 97.25%, respectively, which was similar to previous results (Pala *et al.* 2014). When the residence time remained constant (a residence time of 30 min) and the reaction temperature was varied, the HHV increased from 18.35 MJ/kg to 23.64 MJ/kg, the mass yield decreased from 81.42% to 50.49%, and the energy yield decreased from 87.02% to 69.51%. The HHV of hydrochar obtained at 260 °C for 30 min could be compared with that dry torrefied stem of corn straw at 300 °C for 40 min (20.26 MJ/kg) (Mei *et al.* 2016), and which is approximately equivalent to the heating value of coal (Nizamuddin *et al.* 2015). The hydrochar prepared at 230 °C or 260 °C could be comparable with some of commercial fuels (Yang *et al.* 2016). Meanwhile, when the reaction temperature remained constant and the reaction time was varied, the results were relatively unchanged.

Table 2. The Ultimate Analysis, Heating Value, and Mass and Energy Yields of Corn Straw and Hydrochar

Materials	Carbon (%)	Hydrogen (%)	Nitrogen (%)	Sulfur (%)	Oxygen (%)	HHV (MJ·kg ⁻¹)	Mass yield (%)	Energy yield (%)
CS	43.30±0.29	5.95±0.22	1.21±0.08	0.12±0.02	49.42±0.47	17.17±0.34	-	-
CS170-15	44.72±0.19	6.02±0.01	1.16±0.02	0.07±0.01	48.03±0.24	18.05±0.26	92.51±0.34	97.25±0.14
CS170-30	44.98±0.22	6.00±0.11	1.14±0.07	0.07±0.01	47.81±0.24	18.35±0.35	81.42±0.41	87.02±0.24
CS200-15	46.1±0.23	5.86±0.01	1.32±0.01	0.09±0.01	46.63±0.19	18.83±0.24	74.24±0.24	81.42±0.15
CS200-30	47.47±0.12	5.79±0.02	1.25±0.02	0.10±0.00	45.39±0.16	19.18±0.36	73.84±0.27	82.48±0.24
CS230-15	48.33±0.33	5.72±0.04	1.22±0.03	0.08±0.01	44.65±0.15	19.57±0.24	69.87±0.31	79.64±0.17
CS230-30	49.65±0.32	5.51±0.01	1.38±0.01	0.11±0.01	43.35±0.24	20.51±0.31	64.80±0.21	77.41±0.19
CS260-15	52.40±0.28	5.51±0.14	1.16±0.07	0.14±0.01	40.79±0.34	22.35±0.55	53.11±0.32	69.13±0.44
CS260-30	54.57±0.54	5.84±0.21	1.15±0.10	0.13±0.00	38.31±0.42	23.64±0.38	50.49±0.29	69.51±0.31

Note: Oxygen content was obtained by difference. The values are represented as the mean ± standard deviation (n=3)

CS: Corn straw; CS170-15: Corn straw-170 °C-15 min; CS170-30: Corn straw-170 °C-30 min; CS200-15: Corn straw-200 °C-15 min; CS200-30: Corn straw-200 °C-30 min; CS230-15: Corn straw-230 °C-15 min; CS230-30: Corn straw-230 °C-30 min; CS260-15: Corn straw-260 °C-15 min; CS260-30: Corn straw-260 °C-30 min

It is possible that the subcritical state of water promoted the pyrolysis of the biomass. Under these operating conditions, the temperature appeared to exhibit a stronger effect than the reaction time on hydrothermal carbonization production distributions. The hydrothermal carbonization conditions resulted in an increase in HHV with increasing temperature and residence time. On the contrary, the mass and energy yields decreased.

The Fuel Properties of Hydrochar

The carbon content of hydrochar increased with increasing hydrothermal carbonization temperature and residence time. The carbon content of hydrochar was 49.65% after a residence time of 30 min at 230 °C, with an elevation of 14.67%. Meanwhile, the oxygen content declined to 43.35%, with a reduction of 11.98%. This phenomenon was attributed to the reduction in hydroxyl and carbonyl groups in the form of water during hydrothermal carbonization (Zheng *et al.* 2015). Additionally, the hydrogen, nitrogen, and sulfur contents of the hydrochar minimally varied after hydrothermal carbonization. The ultimate analysis of corn straw and hydrochar indicated that the fuel properties of corn straw were improved after hydrothermal carbonization.

Variation in the atomic H/C and O/C ratios of a sample can be used to efficiently evaluate the fuel properties of solid fuel. Therefore, the atomic H/C and O/C ratios from corn straw and hydrochar were calculated and plotted to obtain the Van Krevelen diagram (Fig. 1). The H/C and O/C ratios of the hydrochars decreased with increasing temperature and residence time, and their ratios were considerably lower than that of the raw corn straw, especially the hydrochar produced at 260 °C for 30 min. As shown in Fig. 1, the atomic H/C and O/C ratios of hydrochar were within the range of 1.63 to 1.28 and 0.81 to 0.53, respectively, which were obviously lower than that of raw corn straw (H/C: 1.65, O/C: 0.86). This phenomenon was attributed to decarbonization, dehydration, and demethanation processes during hydrothermal carbonization. Generally, hydrothermal carbonization can elevate the combustion properties of corn straw.

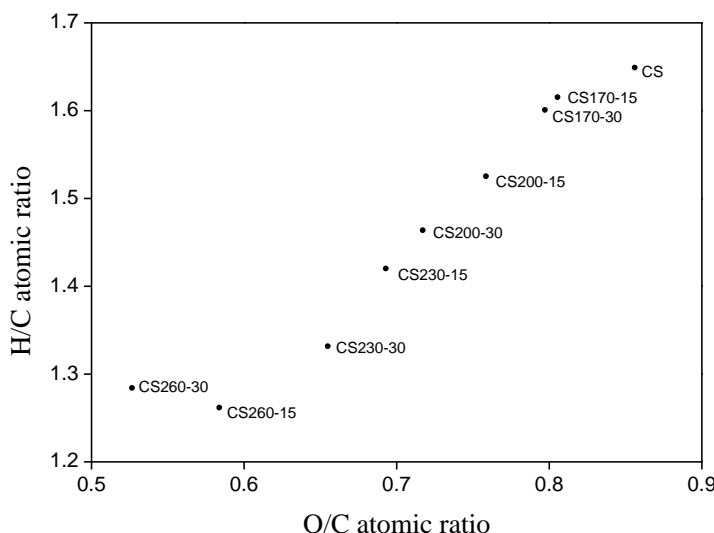


Fig. 1. Van Krevelen diagram of corn straw and hydrochar

SEM Morphology of Corn Straw and Hydrochar

The physical structures of corn straw and hydrochar are shown in Fig. 2 at various temperatures and a 30-min residence time. The images of the samples showed that the

structure varied with increasing temperature. Raw corn straw and hydrochar produced at 170 °C and 200 °C retained their complete structures. Nevertheless, at higher temperatures (230 °C and 260 °C), microspheres and fragmentation appeared. These microspheres and fragmentation were mainly derived from the degradation of cellulose and hemicelluloses (Liang *et al.* 2011). Corn straw contains *ca.* 41.16% cellulose and 28.13% hemicelluloses (Zhong *et al.* 2011), which were mainly decomposed.

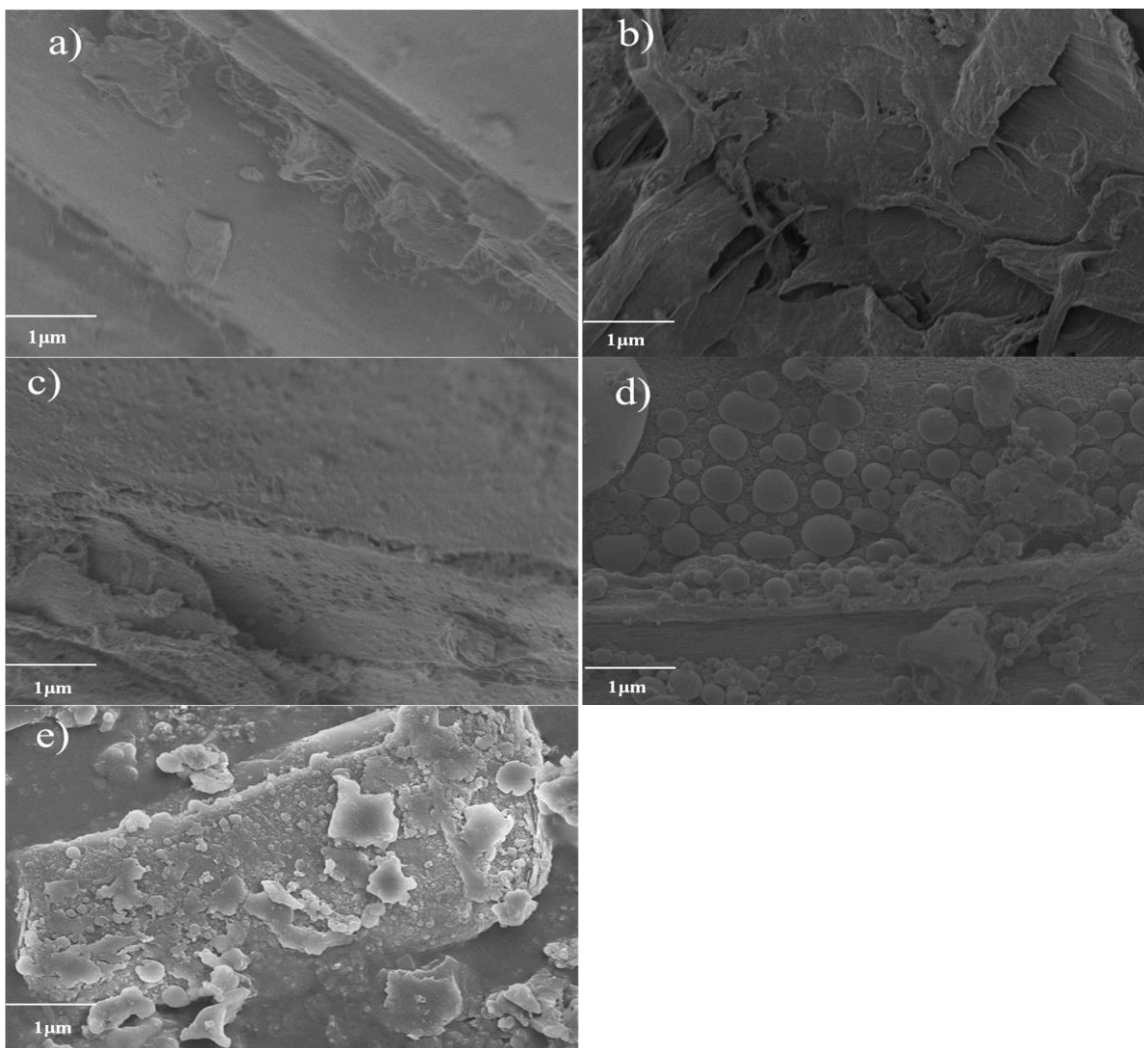


Fig. 2. Scanning electron micrograph images of: a) CS; b) CS170-30; c) CS200-30; d) CS230-30; and e) CS260-30

Hydrophobicity

One of the major limitations for raw biomass is its tendency to absorb moisture from the atmosphere, especially after drying. Biomass with high moisture content can support fungal growth and will most likely rot over time. High moisture content can also cause self-heating of the biomass when stockpiled because of the heat production from oxidation and microbial activity (Kambo and Dutta 2015). Thermal pretreatments are often proposed to improve the hydrophobicity of biomass.

The equilibrium moisture content (EMC) often represents the hydrophobicity of a sample. The results for the hydrophobicity of corn straw and hydrochar solid samples are

shown in Table 3. The hydrophobicity of hydrochar was improved by hydrothermal carbonization and increased with increasing hydrothermal temperature and residence time. Compared with corn straw, the EMC of hydrochar decreased from 5.63% to 1.81% when the relative humidity was 42%, and from 6.89% to 1.97% when the relative humidity was 75%. The amount of moisture biomass absorbs from the air is associated with the compositions of feedstock. Cellulose and hemicelluloses have a strong capacity for water absorption (Vyas *et al.* 2015). Consequently, a reduction in cellulose and hemicelluloses will improve the hydrophobicity of the biomass; thereby, thermal pretreatment by hydrothermal carbonization is warranted.

Table 3. Hydrophobicity of Corn Straw and Hydrochar

Materials	Percentage moisture content	
	RH 42%	RH 75%
CS	5.63±0.15	6.89±0.32
CS170-15	4.82±0.22	6.31±0.15
CS170-30	4.67±0.15	5.14±0.19
CS200-15	3.14±0.22	4.25±0.24
CS200-30	2.83±0.17	4.15±0.17
CS230-15	2.11±0.14	3.31±0.26
CS230-30	1.88±0.24	2.29±0.14
CS260-15	1.80±0.08	2.07±0.21
Cs260-30	1.81±0.11	1.97±0.14

Note: The values are represented as the mean ± standard deviation (n=3)

CS: Corn straw; CS170-15: Corn straw-170 °C-15 min; CS170-30: Corn straw-170 °C-30 min; CS200-15: Corn straw-200 °C-15 min; CS200-30: Corn straw-200 °C-30 min; CS230-15: Corn straw-230 °C-15 min; CS230-30: Corn straw-230 °C-30 min; CS260-15: Corn straw-260 °C-15 min; CS260-30: Corn straw-260 °C-30 min

Based on the aforementioned result, the fuel properties of corn straw were upgraded by hydrothermal carbonization, and the hydrophobicity also improved. Accordingly, the properties of the hydrochar prepared at 230 °C and 30 min were the best.

Combustion Kinetics Parameters of Corn Straw and Hydrochar

Figures 3 and 4 show the resulting TG and DTG curves of corn straw and hydrochar (CS230-30) combustion, with a heating rate of 20 °C/min for corn straw and 10 °C/min, 20 °C/min, and 40 °C/min for hydrochar, respectively.

According to the TG and DTG curves of corn straw and hydrochar, the weight loss mechanism suggested that there were two distinct zones, including the volatile matter and char combustion stages. Meanwhile, the kinetic parameters were calculated by the data corresponding to the different stages. It can be seen that all the hydrochars were less reactive than the raw one at different heating rate. This is explained by the presence of hemicelluloses and cellulose.

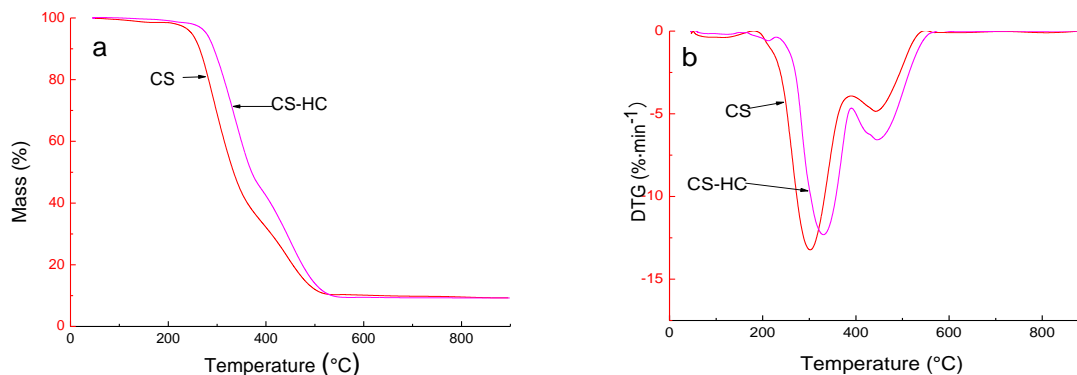


Fig. 3. The a) TG curve and b) DTG curve of corn straw and hydrochar combustion at 20 °C/min

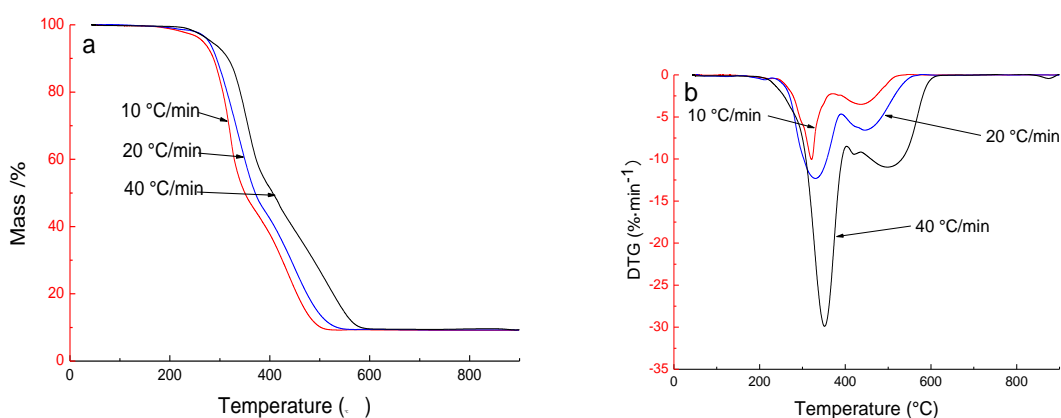


Fig. 4. The a) TG curve and b) DTG curve of corn straw and hydrochar combustion at different heating rates

The determination of kinetic parameters is of great importance to understanding of combustion behaviors of corn straw and hydrochar. The activation energy and the pre-exponential factor are two parameters for evaluating the characteristics of combustion for the production of solid fuel.

Because the TG and DTG curves show the difference in the volatile matter and char combustion stages, the raw data corresponding to different stages in TG and DTG are different, and the kinetic parameters of each stage were determined by linear regression. According to the results of linear regression, using different kinetic mechanisms, the first-order combustion reaction was the most appropriate functional model, with a regression coefficient ranging from 0.930 to 0.976 (Table 4).

The activation energy in the first combustion stage was higher than that in the second combustion stage for all of the samples. Meanwhile, the hydrochar exhibited a relatively higher activation energy (59.5 kJ/mol) compared to raw corn straw (52.7 kJ/mol) at 20 °C/min (Table 4). This was because a portion of the relative compounds in cellulose and hemicelluloses decomposed during hydrothermal carbonization. There was a slight effect on the activation energy of hydrochar during the first combustion stage, while the activation energy decreased from 41.6 kJ/mol to 34.2 kJ/mol in the second combustion stage when the heating rate increased from 10 °C/min to 40 /min.

Table 4. The Kinetic Parameters of Corn Straw and Hydrochar

Materials	Heating rates (°C·min ⁻¹)	Temperature (°C)	<i>E</i> (kJ·mol ⁻¹)	<i>A</i> (min ⁻¹)	R ²
CS	20	250 to 383	52.7	8.18×10 ³	0.930
		396 to 510	29.6	40.2	0.971
CS230-30	10	285 to 369	68.7	9.69×10 ⁴	0.931
		391 to 493	41.6	1.25×10 ²	0.971
CS230-30	20	290 to 386	59.5	1.93×10 ⁴	0.968
		396 to 520	37.7	1.54×10 ²	0.976
CS230-30	40	311 to 402	67.0	1.04×10 ⁵	0.962
		432 to 569	34.2	99.5	0.940

Note: CS: Corn straw; CS230-30: Corn straw-230 °C-30 min

Evaluation of Combustion Performances

The comprehensive combustibility index values were calculated in Table 5 for corn straw and hydrochar prepared at 230 °C and 30 min. Compared with the raw material, the $(dw/dt)_{max}$ of corn straw decreased by 0.92%, and the comprehensive combustibility index decreased by 0.50×10^{-7} at the heating rate of 20 °C/min. This is because corn straw contains higher volatile matter. However, a high volatile matter can cause unstable flame and combustion, leading to energy losses. It is meaningful to produce hydrochar via hydrothermal carbonization. Besides, the comprehensive combustibility index increased from 1.63×10^{-7} to 13.4×10^{-7} when the heating rate increased from 10 °C/min to 40 °C/min (Table 5).

Table 5. The Combustion Characteristic Parameters of Corn Straw and Hydrochar

Sample	Heating rates (°C·min ⁻¹)	<i>T_i</i> (°C)	<i>T_h</i> (°C)	$(dw/dt)_{max}$ (%·min ⁻¹)	$(dw/dt)_{mean}$ (%·min ⁻¹)	S×10 ⁻⁷
CS	20	250	510	13.23	6.46	3.99
CS230-30	10	285	493	10.06	3.86	1.63
CS230-30	20	290	520	12.31	7.12	3.49
CS230-30	40	311	569	29.89	12.90	13.4

Note: CS: Corn straw; CS230-30: Corn straw-230 °C-30 min

CONCLUSIONS

1. The fuel properties of corn straw were upgraded by hydrothermal carbonization, and the properties of the hydrochar prepared at 230 °C and 30 min were optimal. The mass and energy yields of hydrochar were 64.8% and 77.41%, respectively. The carbon content and HHV of hydrochar increased from 43.3% to 49.65% and 17.17 MJ/kg to 20.51 MJ/kg, respectively.
2. The atomic H/C and O/C ratios were elevated under the conditions of 230 °C and 30 min. The HHV, H/C, and O/C of CS230-30 indicated that solid hydrochar from corn straw produced a solid fuel suitable for co-combustion with lignite. The SEM topography of corn straw and hydrochar showed that the decomposition of corn straw

increased with increasing hydrothermal carbonization temperature and residence time. This thermal pretreatment reduced the moisture uptake of solid fuel compared with raw corn straw. The hydrochar samples produced via hydrothermal carbonization exhibited greater hydrophobicity than raw corn straw, according to the EMC of 32% and 75% relative humidity.

3. The kinetic parameters of corn straw and hydrochar during combustion and the comprehensive combustibility index were analyzed by TGA. Two distinct zones were observed for all materials by kinetic parameters calculation. The activation energy of hydrochar in the first and second combustion stages was higher than that of the raw corn straw at 20 °C/min, with the first stage exceeding that of the second stage. The comprehensive combustibility index increased from 1.63×10^{-7} to 13.4×10^{-7} when the heating rate increased from 10 °C/min to 40 °C/min. At 20 °C/min, the comprehensive combustibility index of raw corn straw was greater than that of CS230-30.

ACKNOWLEDGEMENTS

The authors thank the National Science and Technology Support Program of China (2012BAD30801).

REFERENCES CITED

- Abnisa, F., and Daud, W. M. A. W. (2014). "A review on co-pyrolysis of biomass: An optional technique to obtain a high-grade pyrolysis oil," *Energy Conversion and Management* 87, 71-85. DOI: 10.1016/j.enconman.2014.07.007
- Álvarez-Murillo, A., Román, S., Ledesma, B., and Sabio, E. (2015). "Study of variables in energy densification of olive stone by hydrothermal carbonization," *Journal of Analytical and Applied Pyrolysis* 113, 307-314. DOI: 10.1016/j.jaap.2015.01.031
- Benavente, V., Calabuig, E., and Fullana, A. (2014). "Upgrading of moist agro-industrial wastes by hydrothermal carbonization," *Journal of Analytical and Applied Pyrolysis* 113, 89-98. DOI: 10.1016/j.jaap.2014.11.004
- Basso, D., Patuzzi, F., Castello, D., Baratieri, M., Rada, E. C., Weiss-Hortala, E., and Fiori, L. (2016). "Agro-industrial waste to solid biofuel through hydrothermal carbonization," *Waste Management* 47, 114-121. DOI: 10.1016/j.wasman.2015.05.013
- Chen, M., Zhao, J., and Xia, L. (2008). "Enzymatic hydrolysis of maize straw polysaccharides for the production of reducing sugars," *Carbohydrate Polymers* 71(3), 411-415. DOI: 10.1016/j.carbpol.2007.06.011
- Fuertes, A. B., Arbustain, M. C., Sevilla, M., Macia-Agullo, J. A., Fiol, S., López, R., Smernik, R. J., Aitkenhead, W. P., Arce, F., and Macias, F. (2010). "Chemical and structural properties of carbonaceous products obtained by pyrolysis and hydrothermal carbonisation of corn stover," *Soil Research* 48(7), 618-626. DOI: 10.1071/SR 10010

- Fang, X., Jia, L., and Yin, L. (2013). "A weighted average global process model based on two-stage kinetic scheme for biomass combustion," *Biomass and Bioenergy* 48, 43-50. DOI: 10.1016/j.biombioe.2012.11.011
- Garcia-Maraver, A., Perez-Jimenez, J. A., Serrano-Bernardo, F., and Zamorano, M. (2015). "Determination and comparison of combustion kinetics parameters of agricultural biomass from olive trees," *Renewable Energy* 83, 897-904. DOI: 10.1016/j.renene.2015.05.049
- Gao, Y., Yu, B., Wu, K., Yuan, Q., Wang, X., and Chen, H. (2016). "Physicochemical, pyrolytic, and combustion characteristics of hydrochar obtained by hydrothermal carbonization of biomass," *BioResources* 11(2), 4113-4133. DOI: 10.15376/biores.11.2.4113-4133
- Guo, S., Dong, X., Wu, T., Shi, F., and Zhu, C. (2016). "Influence of reaction conditions and feedstock on hydrochar properties," *Energy Conversion and Management* 123, 95-103. DOI: 10.1016/j.enconman.2016.06.029
- Islam, M. A., Auta, M., Kabir, G., and Hameed, B. H. (2016). "A thermogravimetric analysis of the combustion kinetics of karanja (*Pongamia pinnata*) fruit hulls char," *Bioresource Technology* 200, 335-341. DOI: 10.1016/j.biortech.2015.09.057
- Jin, W., Xu, X., Yang, G., Yang, F., and Gang, W. (2014). "Anaerobic fermentation of biogas liquid pretreated maize straw by rumen microorganisms *in vitro*," *Bioresource Technology* 153, 8-14. DOI: 10.1016/j.biortech.2013.10.003
- Jatzwauck, M., and Schumpe, A. (2015). "Kinetics of hydrothermal carbonization (HTC) of soft rush," *Biomass and Bioenergy* 75, 94-100. DOI: 10.1016/j.biombioe.2015.02.006
- Kambo, H. S., and Dutta, A. (2015). "Comparative evaluation of torrefaction and hydrothermal carbonization of lignocellulosic biomass for the production of solid biofuel," *Energy Conversion and Management* 105, 746-755. DOI: 10.1016/j.enconman.2015.08.031
- Liang, J. L., Liu, Y. H., and Zhang, J. (2011). "Effect of solution pH on the carbon microsphere synthesized by hydrothermal carbonization," *Procedia Environmental Sciences* 11, 1322-1327. DOI: 10.1016/j.proenv.2011.12.198
- Libra, J. A., Ro, K. S., Kammann, C., Funke, A., Berge, N. D., Neubauer, Y., Tititici, M., Fühner, C., Bens, O., Kern, J., and Emmerich, K. (2011). "Hydrothermal carbonization of biomass residuals: A comparative review of the chemistry, processes and applications of wet and dry pyrolysis," *Biofuels* 2(1), 71-106. DOI: 10.4155/bfs.10.81
- Lou, B., Wu, S., Wang, X., Ma, K., and Li, M. (2014). "Experimentation and simulation of the combustion of biomass briquettes in southern China," *BioResources* 9(4), 5831-5844. DOI: 10.15376/biores.9.4.5831-5844
- Lu, W., Ding, W., Zhang, J., Zhang, H., Luo, J., and Bolan, N. (2015). "Nitrogen amendment stimulated decomposition of maize straw-derived biochar in a sandy loam soil: A short-term study," *Plos One* 10(7), 0133131. DOI: 10.1371/journal.pone.0133131
- Ma, L., Wang, T., Liu, Q., Zhang, X., Ma, W., and Qi, Z. (2012). "A review of thermal-chemical conversion of lignocellulosic biomass in China," *Biotechnology Advances* 30(4), 859-873. DOI: 10.1016/j.biotechadv.2012.01.016
- Miranda, M. T., Arranz, J. I., Rojas, S., and Montero, I. (2009). "Energetic characterization of densified residues from pyrenean oak forest," *Fuel* 88(11), 2106-2112. DOI:10.1016/j.fuel.2009.05.015

- Mei, Y., Che, Q., Yang, Q., Draper, C., Yang, H., Zhang, S., and Chen, H. (2016). "Torrefaction of different parts from a corn stalk and its effect on the characterization of products," *Industrial Crops and Products* 92, 26-33. DOI:10.1016/j.indcrop.2016.07.021
- Nizamuddin, S., Jayakumar, N. S., Sahu, J. N., Ganesan, P., Bhutto, A. W., and Mubarak, N. M. (2015). "Hydrothermal carbonization of oil palm shell," *Korean Journal of Chemical Engineering* 32(9), 1-9. DOI: 10.1007/s11814-014-0376-9
- Nizamuddin, S., Jaya Kumar, N. S., Sahu, J. N., Ganesan, P., Mubarak, N. M., and Mazari, S. A. (2015). "Synthesis and characterization of hydrochars produced by hydrothermal carbonization of oil palm shell," *Canadian Journal of Chemical Engineering* 93(2), 457-458. DOI: 10.1002/cjce.22293
- Nizamuddin, S., Mubarak, N. M., Tiripathi, M., Jayakumar, N. S., Sahu, J. N., and Ganesan, P. (2015). "Chemical, dielectric and structural characterization of optimized hydrochar produced from hydrothermal carbonization of palm shell," *Fuel*, 163.88-97. DOI: 10.1016/j.fuel.2015.08.057
- Pala, M., Kantarli, I. C., Buyukisik, H. B., and Yanik, J. (2014). "Hydrothermal carbonization and torrefaction of grape pomace: A comparative evaluation," *Bioresource Technology* 161, 255-262. DOI: 10.1016/j.biortech.2014.03.052
- Sait, H. H., Hussain, A., Salema, A. A., and Ani, F. N. (2012). "Pyrolysis and combustion kinetics of date palm biomass using thermogravimetric analysis," *Bioresource Technology* 118, 382-389. DOI: 10.1016/j.biortech.2012.04.081
- Smith, A. M., and Ross, A. (2016). "Production of bio-coal, bio-methane and fertilizer from seaweed via hydrothermal carbonization," *Algal Research* 16, 1-11. DOI: 10.1016/j.algal.2016.02.026
- Thangalazhy-Gopakumar, S., Al-Nadheri, W. M. A., Jegarajan, D., Sahu, J. N., Mubarak, N. M., and Nizamuddin, S. (2015). "Utilization of palm oil sludge through pyrolysis for bio-oil and bio-char production," *Bioresource Technology* 178, 65-69. DOI:10.1016/j.biortech.2014.09.068
- Vyas, D. K., Sayyad, F. G., Khardiwar, M. S., and Kumar, S. (2015). "Physicochemical properties of briquettes from different feed stock," *Current World Environment* 10(1), 263-269. DOI: 10.12944/CWE.10.1.32
- Valverde, V., Pay, M. T., and Baldasano, J. M. (2016). "A model-based analysis of SO₂ and NO₂ dynamics from coal-fired power plants under representative synoptic circulation types over the Iberian Peninsula," *Science of The Total Environment* 541, 701-713. DOI: 10.1016/j.scitotenv.2015.09.111
- Wang, Q., Xu, H., Liu, H., Jia, C., and Zhao, W. (2012). "Co-combustion performance of oil shale semi-coke with corn stalk," *Energy Procedia* 17, 861-868. DOI: 10.1016/j.egypro.2012.02.180
- Wang, X., Hu, Z., Deng, S., Wang, Y., and Tan, H. (2015). "Kinetics investigation on the combustion of biochar in O₂/CO₂ atmosphere," *Environmental Progress and Sustainable Energy* 34(3), 923-932. DOI: 10.1002/ep.12063
- Wang, S., Ru, B., Dai, G., Sun, W., Qiu, K., and Zhou, J. (2015). "Pyrolysis mechanism study of minimally damaged hemicellulose polymers isolated from agricultural waste straw samples," *Bioresource Technology* 190, 211-218. DOI: 10.1016/j.biortech.2015.04.098

- Xiao, L. P., Shi, Z. J., Feng, X., and Sun, R. C. (2012). "Hydrothermal carbonization of lignocellulosic biomass," *Bioresource Technology* 118, 619-623. DOI: 10.1016/j.biortech.2012.05.060
- Yang, W., Wang, H., Zhang, M., Zhu, J., Zhou, J., and Wu, S. (2016). "Fuel properties and combustion kinetics of hydrochar prepared by hydrothermal carbonization of bamboo," *Bioresource Technology* 205, 199-204. DOI: 10.1016/j.biortech.2016.01.068
- Zhong, W., Zhang, Z., Luo, Y., Sun, S., Wei, Q., and Meng, X. (2011). "Effect of biological pretreatments in enhancing corn straw biogas production," *Bioresource Technology* 102(24), 11177-11182. DOI:10.1016/j.biortech.2011.09.077
- Zhao, X., Wang, J., Wang, S., and Xing, G. (2014). "Successive straw biochar application as a strategy to sequester carbon and improve fertility: A pot experiment with two rice/wheat rotations in paddy soil," *Plant and Soil* 378(1-2), 279-294. DOI: 10.1007/s11104-014-2025-9
- Zheng, A., Zhao, Z., Sheng, C., Zhen, H., Zhao, K., Wei, G., Fang, H., and Li, H. (2015). "Comparison of the effect of wet and dry torrefaction on chemical structure and pyrolysis behavior of corncobs," *Bioresource Technology* 176, 15-22. DOI: 10.1016/j.biortech.2014.10.157

Article submitted: July 7, 2016; Peer review completed: August 20, 2016; Revised version received and accepted: August 31, 2016; Published: September 13, 2016.
DOI: 10.15376/biores.11.4.9190-9204